Collision Energy Dependence of Hypertriton Production in Au+Au Collisions at RHIC

Xiujun Li[1,*] , for the STAR Collaboration

[1]University of Science and Technology of China

Abstract. Hypernuclei are bound states of nucleons and at least one hyperon. In particular, the hypertriton ${}^{3}_{\Lambda}$H, a bound state consisting of a proton, neutron and hyperon, is the lightest known hypernucleus. Precise measurements on the energy dependence of ${}^{3}_{\Lambda}$H production will give invaluable information on hypernuclei production mechanisms due to its unique intrinsic properties. The second phase of the Beam Energy Scan (BES-II) at RHIC provides a great opportunity to study hypernuclei production. In these proceedings, we present $p_{\mathrm{T}}-$integrated yields (dN/dy) at mid-rapidity, yield ratios and average transverse momentum ($\langle p_T \rangle$) of ${}^{3}_{\Lambda}$H as a function of collision energy in Au+Au collisions from $\sqrt{s_{\mathrm{NN}}}$ = 3 to 27 GeV. These results are compared with phenomenological model calculations, and physics implications on production mechanism are discussed.

1 Introduction

Despite extensive measurements of light nuclei production in heavy-ion collisions, the precise mechanisms underlying their formation remain an open question. Unlike ordinary nuclei, hypernuclei, which contain strange quarks, offer an additional dimension to these studies, while their production mechanisms are not well understood. The equation-of-state (EoS) with the presence of strangeness is crucial for probing the dense neutron star interiors, but the hyperon-nucleon (Y−N) interaction, essential for constraining this EoS, remains poorly understood [1]. Hypernuclei serve as a natural laboratory to study the Y−N interaction. Precise measurements of hypernuclei properties and production yields can shed light on the production mechanisms and the role of Y−N interactions play at neutron stars densities.

The hypertriton ${}^{3}_{\Lambda}$H, a bound state of a proton, neutron, and Λ hyperon, is the lightest known hypernucleus [2]. A prominent enhancement of the strangeness population factor, $S_3 = {}^{3}_{\Lambda}\mathrm{H}/({}^{3}\mathrm{He} \times \frac{\Lambda}{\mathrm{p}})$, has been proposed as a probe for deconfinement [3]. Detailed studies of the energy dependence of ${}^{3}_{\Lambda}$H production could provide valuable insights into the mechanisms of hypernuclei formation.

Notably, light hypernuclei are predicted by thermal models to be abundantly produced at low collision energies due to the high baryon density [4]. A fixed target mode in the STAR (Solenoidal Tracker At RHIC) experiment was specifically implemented during the BES-II running period to reach lower center-of-mass energies, which corresponds to higher baryon density. The low $\sqrt{s_{\mathrm{NN}}}$, enhanced detector capabilities, and high statistics datasets collected during BES-II offer great opportunity for hypernuclei study.

*e-mail: lixiujun@mail.ustc.edu.cn

2 Analysis Details

The measurements of ${}^{3}_{\Lambda}$H production in this analysis are carried out by utilizing the Au+Au collision datasets in at $\sqrt{s_{NN}}$ = 3.0, 3.2, 3.5, 3.9, 4.5 and 5.2 GeV collected with the FXT mode, and data at $\sqrt{s_{NN}}$ = 7.7, 11.5, 14.6, 19.6 and 27 GeV collected in collider mode from STAR experiment during BES-II . The hypertriton ${}^{3}_{\Lambda}$H is reconstructed via its two-body decay channel (${}^{3}_{\Lambda}\mathrm{H} \rightarrow \pi^{-} + {}^{3}\mathrm{He}$) using the KFParticle package [5]. Particle identification of daughters (π^{-} and ^{3}He) is done by using energy loss information from the Time Projection Chamber (TPC). The decay topology is used for ${}^{3}_{\Lambda}$H reconstruction.

3 Results and discussion

The transverse momentum (p_T) spectra of ${}^{3}_{\Lambda}$H are measured in 0-10% and 10-40% central Au+Au collisions at $\sqrt{s_{NN}}$ = 3 to 27 GeV. Figure 1 provides an example of the p_T spectra of ${}^{3}_{\Lambda}$H at $\sqrt{s_{NN}}$ = 7.7 to 27 GeV, with the dotted lines indicating fits to the data.

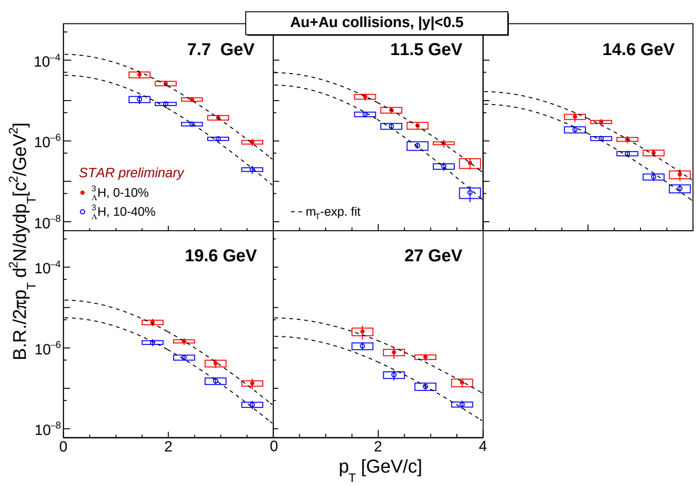

Figure 1. The ${}^{3}_{\Lambda}$H p_T spectra in 0-10% (red circles) and 10-40% (blue circles) central Au+Au collisions. Systematic uncertainties are represented by boxes. The dotted lines are m_T exponential fits to data.

The p_T-integrated yields dN/dy for hypertriton are calculated from the p_T spectra by combining data in the measured p_T range and function-fitting extrapolation in the unmeasured p_T range. Figure 2 presents the energy dependence of the dN/dy for ${}^{3}_{\Lambda}$H at mid-rapidity ($|y| < 0.5$) in 0-10% central Au+Au collisions across a range of $\sqrt{s_{NN}}$ from 3 to 27 GeV. Two predictions, from Ultra-relativistic Quantum Molecular Dynamics (UrQMD)+coalescence [6] and the thermal model [6] are plotted for comparison. In the UrQMD+Coalescence model, the UrQMD transport model generates hadron phase space distributions at freeze-out. A coalescence procedure is then applied, where light nuclei and hypernuclei are formed if the relative momentum and spatial distance of their constituents are within specified thresholds [6]. The thermal model assumes that the chemical freeze-out of light nuclei and hypernuclei happens simultaneously with hadrons [6]. The dN/dy increases as the collision energy decreases, peaking around 3-4 GeV. Both the UrQMD+Coalescence and thermal model calculations capture the overall trend. While the thermal model significantly overestimates the experimental data at all energies, the UrQMD+Coalescence model matches the experimental data below 11.5 GeV.

Figure 3 presents the particle ratios of (hyper)nucleus to hadron (d/p, t/p, and ${}^3_\Lambda\mathrm{H}/\Lambda$) as a function of collision energy. The thermal model results, indicated by dashed/ dash-dotted lines, overestimates the ${}^3_\Lambda\mathrm{H}/\Lambda$ and t/p ratios by a factor of approximately 2, while it successfully describes the d/p ratio in the data. These indicate ${}^3_\Lambda\mathrm{H}$ and triton (t) yields are not in equilibrium and fixed at chemical freeze-out along with other light hadrons.

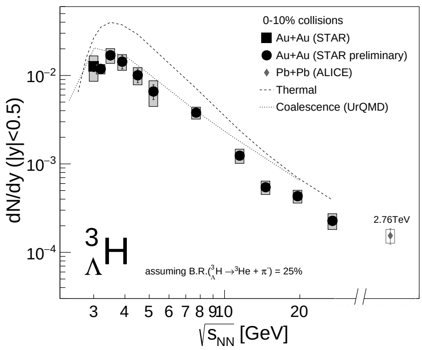

Figure 2. Measured mid-rapidity yields of ${}^3_\Lambda\mathrm{H}$ in 0-10% central Au+Au collisions as function of the center of mass collision energy [7, 8]. The dashed line is from thermal model calculations [6]. The solid line is from transport model calculations with coalescence as an afterburner [6].

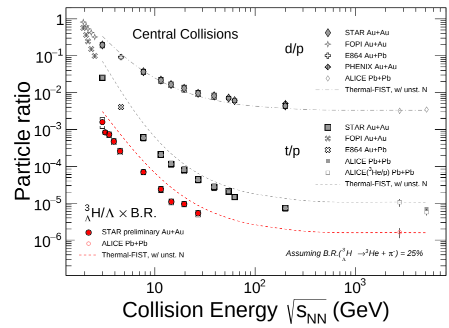

Figure 3. d/p, t/p, and ${}^3_\Lambda\mathrm{H}/\Lambda$ yield ratios in 0-10% central Au+Au collisions as function of the center of mass collision energy. The thermal model results are shown by dashed and dash-dotted lines [6]. Experimental measurements are shown as symbols [9, 10].

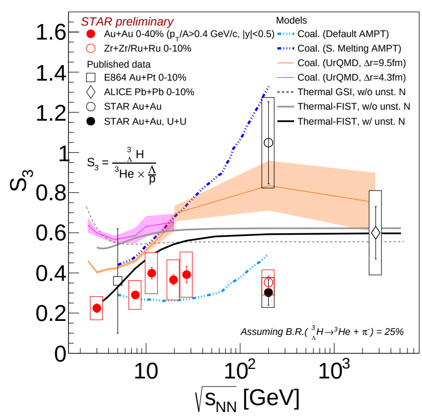

Figure 4. Energy dependence of S_3 from experiments [8, 11–13] and models [3, 4, 6]. The UrQMD+coalescence results with $\Delta r = 9.5$ fm are shown as orange line, while the results of Δr= 4.3 fm are shown as magenta line [6]. The black and grey solid lines correspond to thermal model with/without feed down from unstable nuclei.

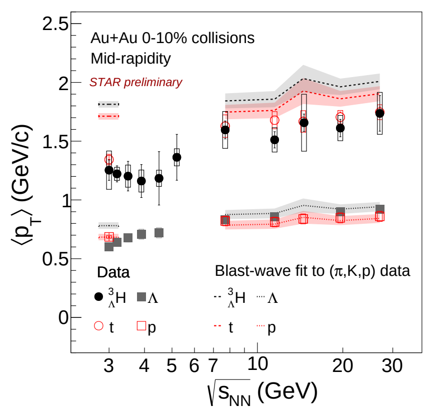

Figure 5. Energy dependence of $\langle p_T \rangle$ for ${}^3_\Lambda\mathrm{H}$, t, Λ, and p in 0-10% most central collisions. In addition, the calculations by fitting the experimental spectra of π, K, p with a blast-wave model are shown as the dashed/solid lines corresponding to the marker color.

Figure 4 presents the energy dependence of the strangeness population factor S_3 from experimental data and compares them with predictions from coalescence and thermal model approaches. The measured S_3 shows a mild increasing trend from $\sqrt{s_{\mathrm{NN}}} = 3$ GeV to 2.76 TeV. If feed down from unstable nuclei to stable protons and $^{3}\mathrm{He}$ is included in the thermal model, the S_3 is reduced and provides a better description of the experimental measurements. In the UrQMD+coalescence results, the energy dependence of S_3 exhibits sensitivity to the coalescence parameter source radius (Δr), possibly due to the difficulty in forming ${}^{3}_{\Lambda}\mathrm{H}$ with a large radius in smaller systems [6].

Figure 5 shows the energy dependence of $\langle p_T \rangle$ of hypertritons, tritons, Λ, and protons in 0-10% central Au+Au collisions from $\sqrt{s_{\mathrm{NN}}} = 3$ to 27 GeV. The $\langle p_T \rangle$ of ${}^{3}_{\Lambda}\mathrm{H}$ and t shows a similar energy-dependence trend. The blast-wave fit using measured kinetic freeze-out parameters from light hadrons (π, K, p) slightly overestimates the $\langle p_T \rangle$ for both ${}^{3}_{\Lambda}\mathrm{H}$ and t. It suggests that ${}^{3}_{\Lambda}\mathrm{H}$ and t do not follow same collective expansion as light hadrons, indicating that ${}^{3}_{\Lambda}\mathrm{H}$ and t decouples at different times compared to light hadrons.

4 Summary and outlook

In summary, we carry out the energy dependence study of hypertriton yields in Au+Au collisions from $\sqrt{s_{\mathrm{NN}}} = 3$ to 27 GeV in the high-baryon-density region. The UrQMD+Coalescence calculations are consistent with data, but the thermal model with the freeze-out parameters determined by the light hadron yields over-predicts hypertriton yields. The over-predictions of the ${}^{3}_{\Lambda}\mathrm{H}/\Lambda$ yield ratio by the thermal model, and the $\langle p_T \rangle$ of ${}^{3}_{\Lambda}\mathrm{H}$ by blast-wave model parametrized from light hadron data, suggest that the ${}^{3}_{\Lambda}\mathrm{H}$ is likely formed at or decouples from the system at a different temperature compared to the light hadrons.

The results in these proceedings utilize only a subset of the BES II datasets. STAR collected 2 billion Au+Au events at $\sqrt{s_{\mathrm{NN}}} = 3$ GeV in Run 21, and is projected to collect 18 billion Au+Au events at $\sqrt{s_{\mathrm{NN}}} = 200$ GeV in Run 23-25, much larger than the datasets presente in these proceedings. The huge datasets would enable precise light hypernuclei measurements and offer great opportunity to the measurements of heavier hypernuclei with A>3.

References

[1] D. Chatterjee, I. Vidana, Eur. Phys. J. A **52**, 1 (2016)
[2] J. Chen, X. Dong, Y.G. Ma, Z. Xu, Sci. Bull. **68**, 3252 (2023)
[3] S. Zhang et al., Phys. Lett. B **684**, 224 (2010)
[4] A. Andronic et al., Phys. Lett. B **697**, 203 (2011)
[5] X.Y. Ju et al., Nucl. Sci. Tech. **34**, 158 (2023)
[6] T. Reichert et al., Phys. Rev. C **107**, 014912 (2023)
[7] M.S. Abdallah et al. (STAR Collaboration), Phys. Rev. Lett. **128**, 202301 (2022)
[8] J. Adam et al. (ALICE Collaboration), Phys. Lett. B **754**, 360 (2016)
[9] M.I. Abdulhamid et al. (STAR Collaboration), Phys. Rev. Lett. **130**, 202301 (2023)
[10] M.I. Abdulhamid et al. (STAR Collaboration) (2023), `arXiv:2311.11020`
[11] T.A. Armstrong et al. (E864 Collaboration), Phys. Rev. C **70**, 024902 (2004)
[12] B. Abelev et al. (STAR Collaboration), Science **328**, 58 (2010)
[13] M.I. Abdulhamid et al. (STAR), Nature **632**, 1026 (2024)